Dynamics of Atomtronic Battery

A Major Qualifying Project Report

submitted to the Faculty

of the

WORCESTER POLYTECHNIC INSTITUTE

in partial fulfillment of the requirements for the

Degree of Bachelor of Science

by

Hongji Yu

Advisors: Alex Z. Zozulya, B.S. Tilley

April 28, 2016

Abstract

Atomtronics studies cold atom analogues of electronic circuits. An ultra-cold Bose gas cloud trapped in a specially shaped trap can serve as a "battery" for such a circuit. We investigate the behavior of this system at different loads. We first perform a bifurcation analysis with respect to the adjustable out-coupling parameter and find a domain where stable solutions exist, as well as a range of initial conditions that converge to stable equilibria. We also look at the relation between the load current and chemical potential, which gives the I-V relation of the battery, and find that the model resembles an electronic battery well at low loads, but shows negative resistance at high loads. Finally we look at a few typical dynamic simulations of the system when the out-coupling strength varies in time.

Contents

Acknowledgements

First I would like to give my sincerest thanks to my MQP advisors, Professor Alexei Zozulya and Professor Burt Tilley for their assistance and feedback throughout the project. Their great advice and active guidance are what made it possible for me to carry this project to the end.

I would also like to thank my family and friends, whose love and support helped me survive and thrive against various challenges and pressure throughout my college carrier.

1 Introduction

1.1 Atomtronics and Bose-Einstein condensate

Atomtronics is an emerging field of physics that studies analogues of electronic circuits and devices with ultra-cold atoms instead of electrons as current carriers [Seaman et al., 2007]. In atomtronics, we use bosonic atoms that are supercooled to form Bose-Einstein condensates as current carriers. Bose-Einstein condensate is a state of matter that forms at extremely low temperatures.

Microscopic particles carry an intrinsic form a angular momentum called spin. In quantum mechanics, angular momenta are quantized, meaning that they can only take discrete values, that is, integer or half integer multiples of the reduced Planck constant $\hbar$ [Sakurai and Napolitano, 2014]. Unlike orbital angular momenta, which are analogous to the classical angular momenta carried by bodies rotating about an axis and can only be integer multiples of $\hbar$, they are not caused by such motions, and can be integer and half integer multiples of $\hbar$. Particles can be classified by their spin. Those carrying half integer spin are called fermions, and those carrying integer spin are called bosons. Fermions obey the Pauli exclusion principle, meaning that there cannot be two identical fermions occupying the exact same state, while bosons are not subject to such limitations. This results in their vastly different behavior when they congregate in large numbers [Pathria and Beale, 2011].

Since bosons can occupy the same quantum states, when the temperature is extremely low (often much less than $1\,\mathrm{K}$), a significant portion of an ensemble of bosons can gather in the lowest energy state, forming Bose-Einstein condensate (BEC) [Pathria and Beale, 2011, pp. 191-199]. Thus macroscopic quantum phenomena such as superfluidity and quantized vortices can be observed [Pethick and Smith, 2002].

Using Bose-Einstein condensate as the current carrier has various benefits and applications. First of all since atoms are electrically neutral, and the interaction between atoms and an external electromagnetic field is much weaker than that between electrons and an external field, atomtronic circuits are much less susceptible to interference. At the same time, we can exploit the magnetic interaction to build atomtronic devices for high accuracy magnetic field sensing Zozulya and Anderson [2013], Seaman et al. [2007]. Various devices that resemble electronic devices can be built for atomtronic circuits, such as capacitors, diodes, and transistors [Lee et al., 2013, Seaman et al., 2007, Pepino et al., 2009, Stickney et al., 2007].

In this project, we look at a system of ultra-cold atoms that imitates a battery, which serve both as a source of atoms and a source of power in an atomtronic circuit.

1.2 Ultra-cooling

To form Bose-Einstein condensates, one must be able to achieve extremely cold temperature. As a point of reference, the Nobel Prize winning experiment in which BEC was first observed saw the formation of it starting at around $200\,\mathrm{nK}$[Cornell and Wieman, 2002]. To obtain such a result, one must use a combination of methods to cool down the system.

In the first stages, laser cooling methods are used. These methods exploit the interaction of atoms with light. The most common method used is Doppler cooling [Pethick and Smith, 2002, pp. 60 - 61]. Atoms can absorb lights at specific frequencies, gaining energy from them, and be excited to a higher energy level. Then the atom may spontaneously emit a photon, and drop down to the original lower state. In this process, the atom also gains and then loses the momentum carried by the photon. Doppler cooling exploits this interaction and the fact that the frequencies of light shift when observed from a moving frame of reference. In the process, laser is applied in two opposite

directions on the same collection of atoms. The frequency of the laser is adjusted to be slightly lower than the required frequency to trigger a transition. Thus in the reference frame of the atoms moving away from the trap, due to the Doppler effect the laser pointing opposite the direction of motion has higher frequency than in the lab frame, becoming closer to the frequency needed to excite the atoms. This increases the probability of exciting an atom moving away from the trap, and when it is excited, it gains the momentum from the photon moving opposite it, thus slowing it down. Afterwards the atom may emit a photon in a random direction, however overall the net momentum of the system in the outwards direction is reduced.

Doppler cooling can cool atoms to much less than $1\,\mathrm{K}$, but this is not enough for the formation of Bose-Einstein condensate [Pethick and Smith, 2002, p. 81]. To cool it further, the technique of evaporative cooling is used [Pethick and Smith, 2002, pp. 96 - 100]. It is done by gradually lowering the potential barrier that traps the atoms, so that the atoms carrying highest energy are allowed to escape. Then the remaining atoms collide and redistribute their energy, achieving an overall colder equilibrium state. This can eventually get the atoms to cold enough temperature to create BEC.

1.3   Formulation

A further cooling mechanism used in our battery model is introduced by Roos et al. [2003], which involves continuously loading a trap with cold atoms. In this mechanism, particles are injected into a cigar shaped potential well. The incoming atoms enter in the longitudinal direction (z direction) where the trap is also much wider. The potential barrier is designed to be lower in the z direction at U_z than in the other two directions (collectively denoted by the $\perp$ subscript) at $U_\perp$. We also require the trap to be much higher in the opposite direction of where the incoming atoms enter, so
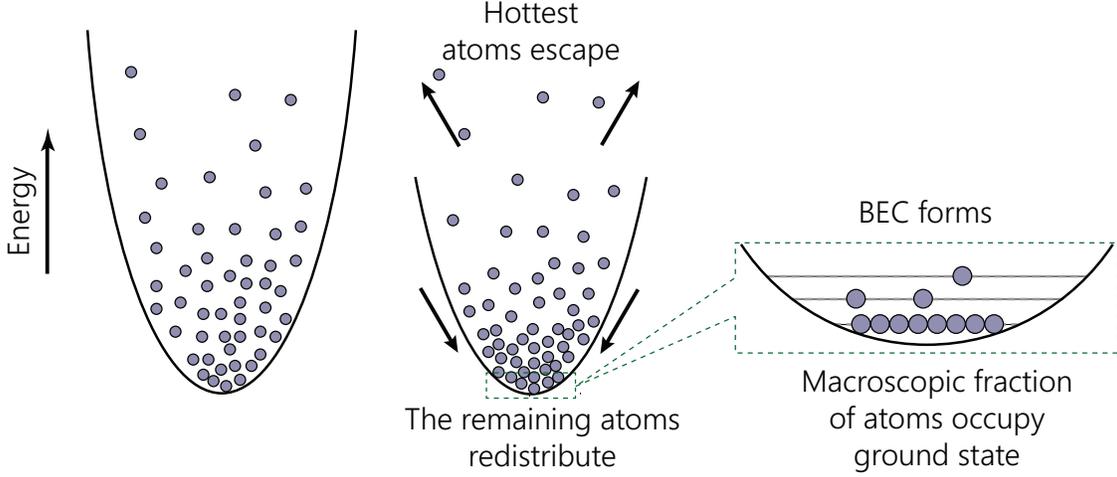
Figure 1: Illustration of evaporative cooling.

the confinement frequency in z direction (f_z) is much smaller than that in the transverse directions ($f_\perp$).

After the atoms in the potential well collide with each other, they may obtain enough energy at certain probabilities to leave the trap. We can find that the probability of an atom leaving the trap in the transverse directions after a collision is

$$p_\perp \approx 2e^{-\eta_\perp} ,$$

where $\eta_\perp = \frac{U_\perp}{kT}$, with T being the temperature. The average excess energy carried away by these atoms is $\kappa_\perp kT$, where $\kappa_\perp$ is around 2.0. Similarly the probability of leaving the trap after collision in the z direction is

$$p_z \approx 0.14e^{-\eta_z}\frac{f_z}{\gamma} ,$$

where $\eta_z = \frac{U_z}{kT}$, and γ is the average collision rate, which can be expressed as

$$\gamma = 32\pi^2 \zeta(3/2)\frac{m(a_s kT)^2}{h^3} .$$

Here m is the atomic mass of the atoms in the trap, a_s is the s-wave scattering length, which
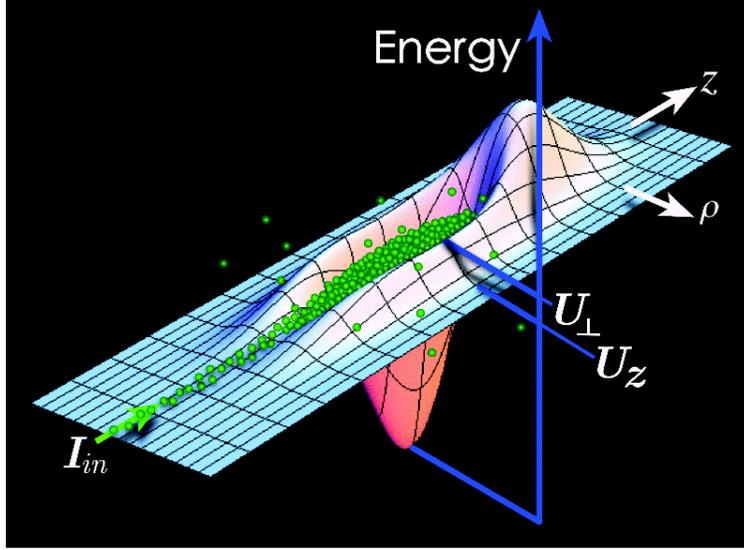
7

Figure 2: Illustration of the atomtronic battery.

characterizes the strength of interaction between the atoms. Atoms leaving in the z direction will carry away $\kappa_z kT$ of energy from the trap on average, with $\kappa_z \approx 2.9$.

The height of the potential barrier in the longitudinal and transverse direction can be adjusted so that we have the maximum number of atoms inside the trap.

When the trap parameters are optimal, Bose-Einstein condensate will form in the trap. Under such conditions, the flow rate of atoms condensing from the thermal cloud into the BEC can be expressed as

$$I_c = \frac{(8\pi)^2 m (a_s kT)^2}{h^3} \frac{\mu_{\text{ex}}\mu_a}{kT} N_a \,,$$

where μ_{ex} and μ_a are the chemical potentials of the thermal atoms and BEC, respectively, and N_a is the number of atoms in the condensate. Under the Thomas-Fermi approximation, we can express the chemical potential of the BEC as

$$\mu_a = \frac{15^{2/5}}{2} \left(\frac{N_a a_s}{\overline{a}} \right)^{2/5} h\overline{f} \,, \tag{1}$$

where $\overline{f} = (f_\perp^2 f_z)^{1/3}$ is the average confinement frequency, and $\overline{a} = \sqrt{\frac{h}{4\pi^2 m\overline{f}}}$. The energy and the

chemical potential of the atoms can also be expressed by

$$E_{\text{ex}} = 3kT \left(\frac{kT}{h\overline{f}}\right)^3 \left[\zeta(4) + 3\frac{\mu_{\text{ex}}}{kT}\zeta(3)\right] ,$$

and

$$\mu_{\text{ex}} = \frac{kT}{\zeta(2)} \left[N_{\text{ex}}\left(\frac{h\overline{f}}{kT}\right)^3 - \zeta(3)\right] .$$

Here N_{ex} is the number of atoms in the thermal cloud.

Now assuming atoms are injected into the potential well at a rate of I_{in}, and on average carry $(1+\epsilon)U_z$ energy, we can write down the conservation equations of the non-condensed atoms,

$$\frac{dN_{\text{ex}}}{dt} = I_{\text{in}} - (p_\perp + p_z)\gamma N_{\text{ex}} - I_c \tag{2}$$

$$\frac{dE_{\text{ex}}}{dt} = I_{\text{in}}(1+\epsilon)U_z - p_z(U_z + \kappa_z kT)\gamma N_{\text{ex}} - \mu_a I_c \tag{3}$$

In these equations, the first terms account for the number and energy of incoming atoms. The second terms describe the number of atoms leaving the trap after gaining enough energy from a collision, and the energy carried away by these atoms. The last terms result from the condensation of thermal atoms into the BEC.

1.4   The atomtronic battery

With the cooling mechanism given above, we can out-couple the BEC forming in the trap into the atomtronic circuit, thus making this system into a source of energy and BEC for an atomtronic circuit. To fully describe the dynamics of the system we need an equation that accounts for the outcoupling as well. Suppose the BEC is outcoupled at the rate

$$I_l = \gamma_a N_a ,$$

where γ_a is the out-coupling strength that we adjust, we can also write down the rate of change of the atoms in the BEC. Assuming the outcoupling mechanism only interacts with the BEC but
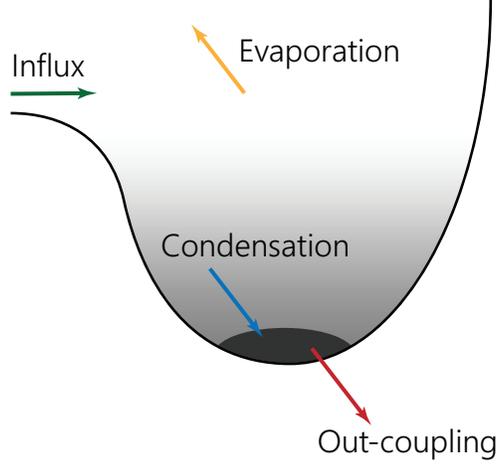
Figure 3: Various flows of atoms and energy in the system.

not the thermal atoms, (2) and (3) are still true. Thus we have the following set of conservation equations,

$$\frac{dE_{\text{ex}}}{dt} = I_{\text{in}}(1 + \epsilon)U_z - p_z(U_z + \kappa_z kT)\gamma N_{\text{ex}} - \mu_a I_c \,,$$

$$\frac{dN_{\text{ex}}}{dt} = I_{\text{in}} - (p_\perp + p_z)\gamma N_{\text{ex}} - I_c \,,$$

$$\frac{dN_a}{dt} = I_c - \gamma_a N_a \,. \tag{4}$$

We can reduce the system to only contain three dynamic variables, with a few experimental parameters left for us to adjust. For our analysis of the dynamics, we shall use the temperature T, the thermal atom number N_{ex} and BEC atom numbers N_a as the state variables.

1.5 Parameters and normalization

In the calculation we are performing here, we use the following values for experimental setup, $\epsilon = 0.7, f_z = 100\,\text{Hz}, f_\perp = 2000\,\text{Hz}$. The s-wave scattering length of rubidium is $a_s = 100.4a_0 = 5.313\,\text{nm}$, where a_0 is the Bohr radius.

When the load on the battery is zero ($\gamma_a = 0$), we can solve for its steady state. Introducing

the threshold flux,

$$I_{\text{th}} = \left(\zeta(3)[p_\perp + p_z]\gamma \left(\frac{kT}{h\overline{f}} \right)^3 \right)_{\text{zero load}},$$

which is the influx of atoms when the BEC is just about to form, we can express the variables representing flow of atoms, such as I_{in} and I_l in the unit of I_{th}, reducing them to the dimensionless form, $i = I_{\text{in}}/I_{\text{th}}$ and $l = I_l/I_{\text{th}}$. Zozulya and Anderson [2013] also introduced reference values for temperature and atom numbers, which are their steady state values at zero load, and in the limit $U_\perp \gg U_z$,

$$kT_0 = \frac{\epsilon U_z}{\kappa_z} , \tag{5}$$

$$N_0 = \left(\frac{I_{\text{in}}}{p_z \gamma} \right)_{\text{zero load}} = 1.14 \frac{I_{\text{in}}}{f_z} e^{\kappa_z/\epsilon} . \tag{6}$$

We can now normalize the dynamic variables, and use $\tau = T/T_0, n_{\text{ex}} = N_{\text{ex}}/N_0, n_a = N_a/N_0$ in our calculation. Using this temperature, we can also reduce the variables with units of energy, so that $u_\perp = U_\perp/kT_0$, $u_z = U_z/kT_0$, $m_{\text{ex}} = \mu_{\text{ex}}/kT_0$, and $m_a = \mu_a/kT_0$.

Finally, we normalize the time variable to units of $1\,\text{s}$, giving a dimensionless time variable that has the same value as real time, which we still denote using t. Consequently, the original out-coupling constant γ_a which has units of frequency now becomes dimensionless.

Now the only parameters left undetermined are γ_a, i, u_z and $u_\perp$. We treat γ_a as a free parameter, and hold i fixed. In this report, a detailed analysis is performed at $i = 1.1$, but the qualitative properties of the system is the same for higher values of i, as we shall see. By (5) we have $u_z = \kappa_z/\epsilon$, and its absolute value is calculated from (6) by requiring that the threshold number of thermal atoms at zero load be $N_{\text{ex}} = 10^6$. For $u_\perp$, we find the optimal value such that at zero load, the steady state value of the temperature is minimal. The result is $u_\perp = 6.5435$.

It is worth noting that even when the optimization of transverse trap height $u_\perp$ is done at a

11

different influx, the optimal trap height and the corresponding values of $t(0)$ and $n(0)$ change very little. According to Zozulya and Anderson [2013], the load also has little effect on the optimization. Thus we use this value of $u_\perp$ throughout the following computations.

2   Stability and bifurcation analysis

With all the parameters fixed, only allowing γ_a to be adjusted, we have an autonomous system of ordinary differential equation that contains one free parameter. Noting that the factors p_z and $p_\perp$ have exponential dependence on the reciprocal temperature, we have a very stiff system.

Using AUTO, a powerful software package that performs stability and bifurcation analysis [Doedel and Oldeman, 2012], we can calculate all the equilibrium states of the equation at different values of the out-coupling parameter.

We can produce the following bifurcation diagrams for all three dynamic variables. Since we are most concerned with the behavior of the BEC in the trap, we shall focus on the behavior of n_a.

From the figure we can see that when γ_a is between 0 and $\gamma_{\text{fold}} = 0.1803$, we have two equilibrium solutions for the system at each γ_a, and the two branches solutions join at a fold. Part of the solution curve is stable, represented by the solid line, and part is unstable, represented by the dashed line. The transition from stable to unstable happens at $\gamma_{\text{Hopf}} = 0.1515$, and is a subcritical Hopf bifurcation. Thus limit cycles exist for $\gamma_a < \gamma_{\text{Hopf}}$, and are unstable. The limit cycles are plotted by the maximum value of the state variables in a period.

Looking further into the limit cycles, we can see that the period increases as we decrease γ_a from the critical point. At $\gamma_{\text{hom}} = 0.1481$, the period goes to infinity, and the limit cycles join with the unstable equilibrium, and becomes a homoclinic orbit.

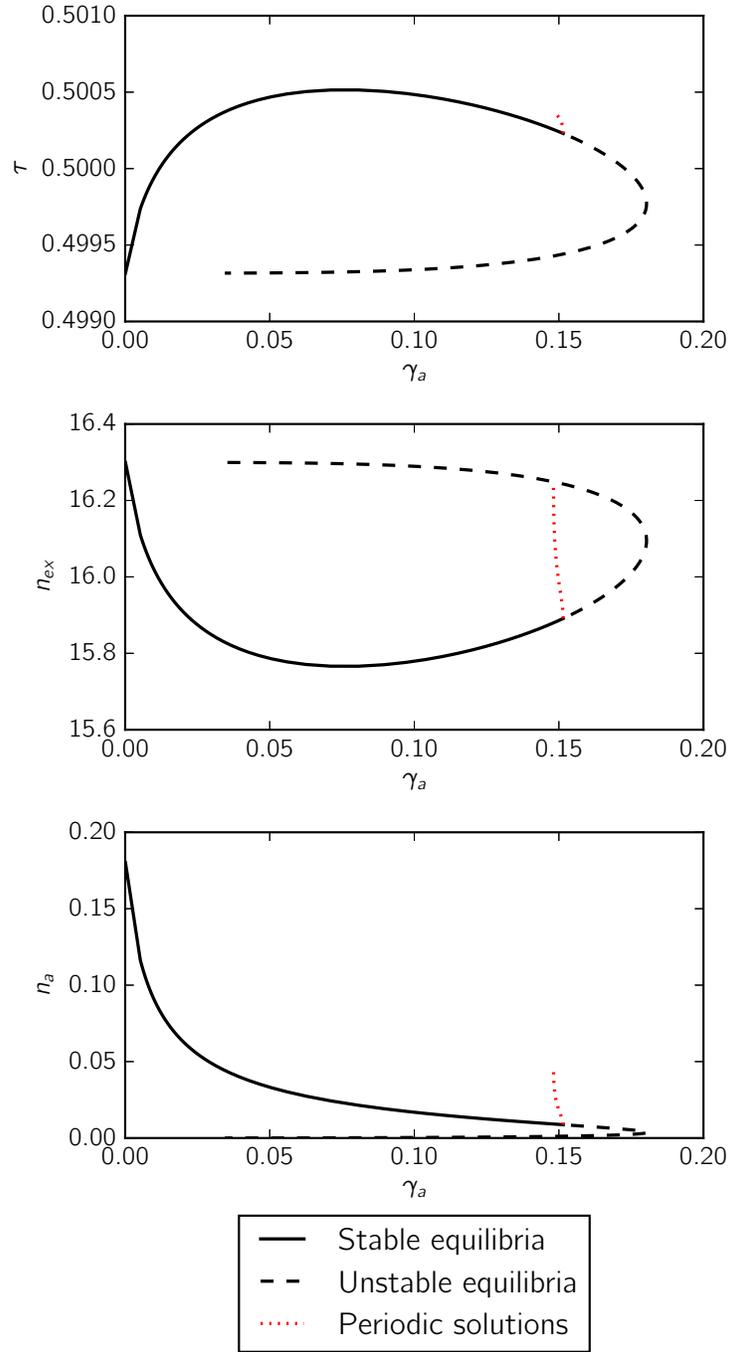Since the limit cycles are unstable, they effectively give the domain of attraction to the stable

Figure 4: Bifurcation diagram of the state variables τ, n_{ex}, and n_a. Periodic solutions are plotted by their maximum values.
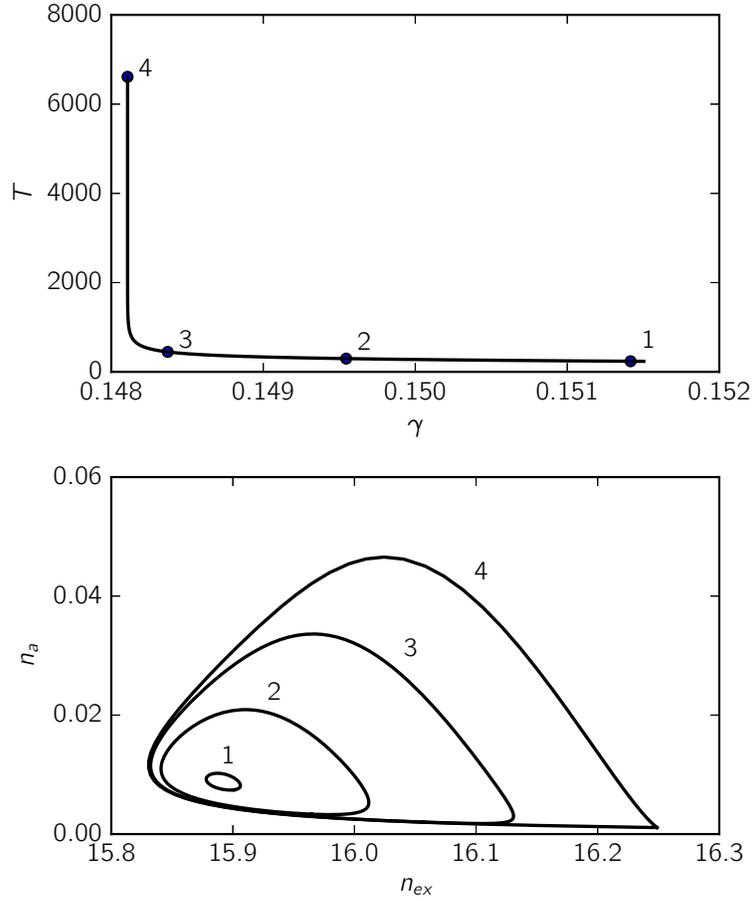
Figure 5: (Top) The period of limit cycles at different out coupling strength. (Bottom) A few labeled solutions graphed in the n_a-n_{ex} phase space. At $\gamma_{\text{hom}} = 0.1481$ the limit cycle becomes a homoclinic cycle (label 4), and is connected to the unstable equilibrium.

equilibria. Thus all initial conditions inside the limit cycle converge to the stable equilibrium, and all outside result in depletion of the BEC. This in turn tells us about the voltage and current rating of the battery.

Using the ode45s toolbox in MATLAB, we can simulate transient solutions with typical initial conditions. Here we plot the n_a-n_{ex} phase space trajectories of these solutions. We can see that when the out-coupling strength is too high, or when the initial condition is too far from equilibrium,
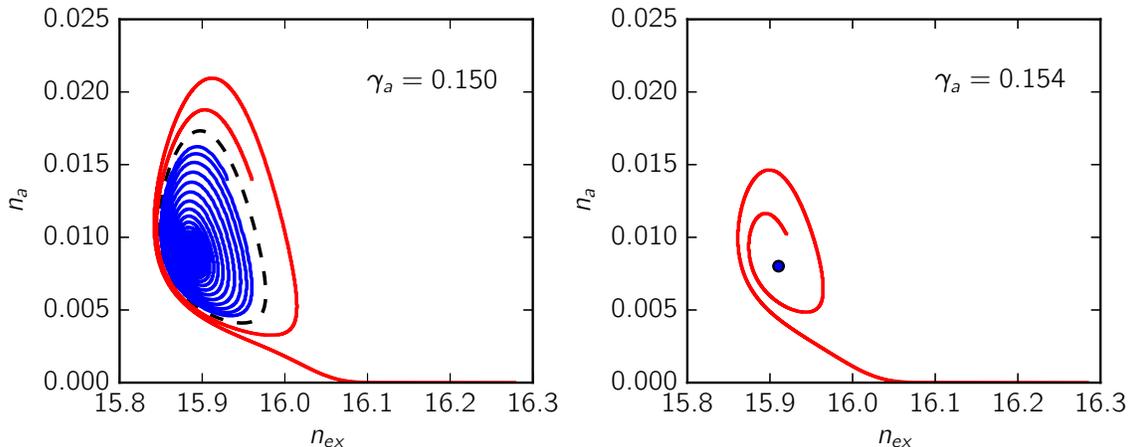
Figure 6: (Left) A limit cycle (dotted line) and two dynamic solutions in n_a-n_ex phase space in the subcritical region. Red line is a solution where the BEC is depleted, and the blue line is a solution that converges to the stable equilibrium. (Right) A dynamic solution when out-coupling strength is supercritical. Red line is a solution where the BEC is depleted. The dot marks the unstable steady state.

the BEC is drained. The graph on the left shows the subcritical situation. The blue line shows convergence onto the stable equilibrium, the red line shows draining of the BEC. The limit cycle (dotted line) separates these two types of solutions.

If we choose a different value for the influx of atoms into the trap to let cold atoms be injected at a higher rate, the number of atoms in the BEC will become much larger, while the thermal atom number remains largely the same (Figure 8). As an example, we show the bifurcation diagrams for $i = 2.0$ in Figure 7. The system exhibits essentially the same dynamic behavior. There are still two branches of steady state solutions, and a transition from stable to unstable steady states happens on one of the branches. The transition is still a subcritical Hopf bifurcation. A family of unstable limit cycles have increasing period as outcoupling strength decreases from the critical value, and
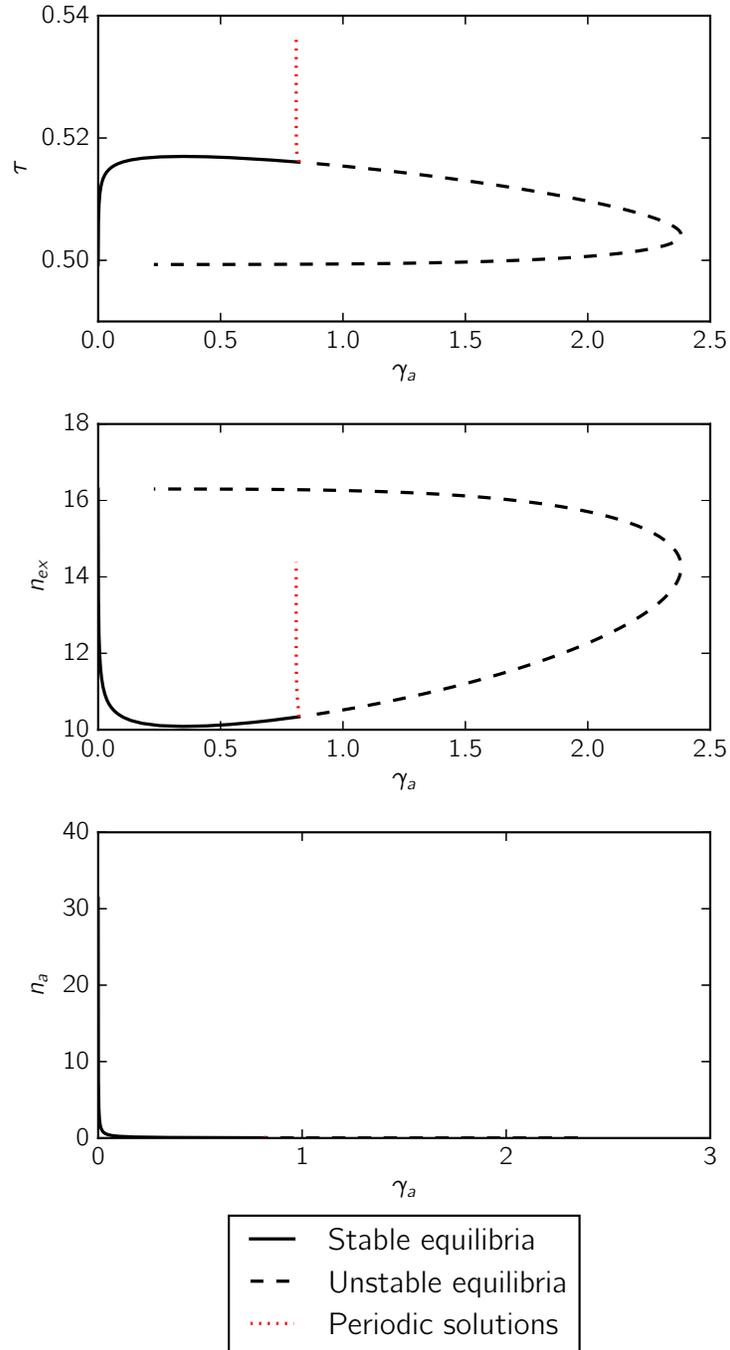
Figure 7: Bifurcation diagram of the state variables τ, n_{ex}, and n_a, when influx $i = 2$. Periodic solutions are plotted by their maximum values.
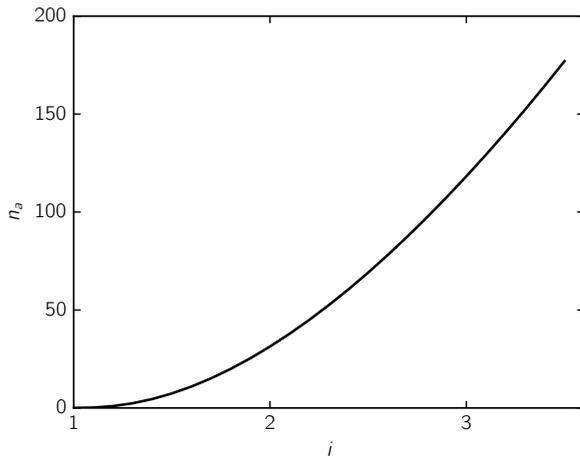
eventually become a homoclinic orbit.

Figure 8: Increasing steady state value of n_a at zero load as influx i increases.

3 Battery

In electronics, to characterize a circuit component, we would measure the current-voltage characteristic. For a power source or battery, it is done by attaching an adjustable load to it, and measuring the current that flows through the load and the voltage across the load. Repeating these measurements at different loads, we have the current-voltage characteristic, which can be used to assess the internal structure of the battery. We do the same for our battery model, where the chemical potential of the BEC is the voltage, and the output current of BEC is the current.

For each stable steady state, we can use the state variables to calculate the chemical potential of the BEC and the out-going flux of the BEC, and then use these data to compute the output power of the battery as well.

From Figure 9 we can see that at lower output, the battery has an approximately linear current-voltage characteristic, which resembles a simple voltage source with inner resistance. This is in
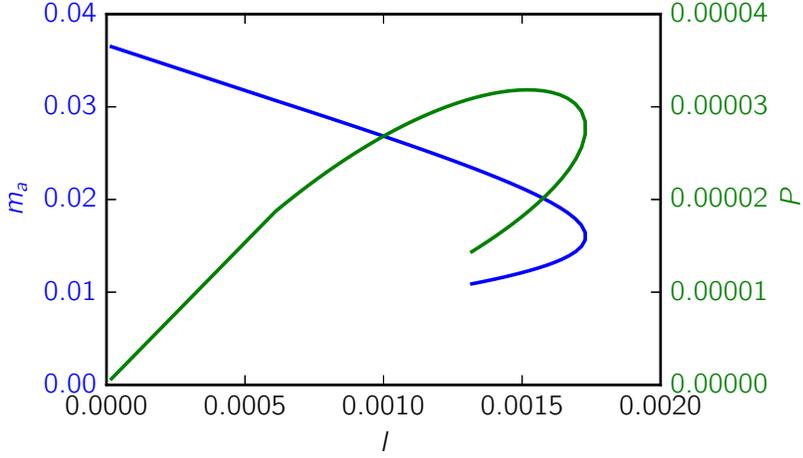
17

Figure 9: Current (l) voltage (m_a) relation of the battery (blue line), and power output (P) at different load voltage (green line).

accordance with the model used by [Zozulya and Anderson, 2013]. However, as the load increases, the m_a-l curve becomes multi-valued. Thus at a given output current, the system can be in two possible working states with different output voltage and output power. This peculiarity is due to the relation between l and γ_a increases. As we can see from Figure 10, as we increase the out coupling strength, the output current first increases then decreases. This behavior can be anticipated from the structure of the I_l term in (4). Since $I_l = \gamma_a N_a$, and N_a decreases as γ_a increases, we can expect their product to increase first then decrease as we increase γ_a. Moreover, according to (1) m_a has a power-law dependence on n_a, thus it decreases monotonously as γ_a grows. This means that the l-m_a relation must be non-monotone, which results in the current-voltage relation we see in Figure 9.

If we increase the influx i to 2.0, the general properties of the battery remain the same, but both output current and output voltage greatly increases. The battery remains linear when the output current is relatively low, and the two-state region occurs much later in the admissible range
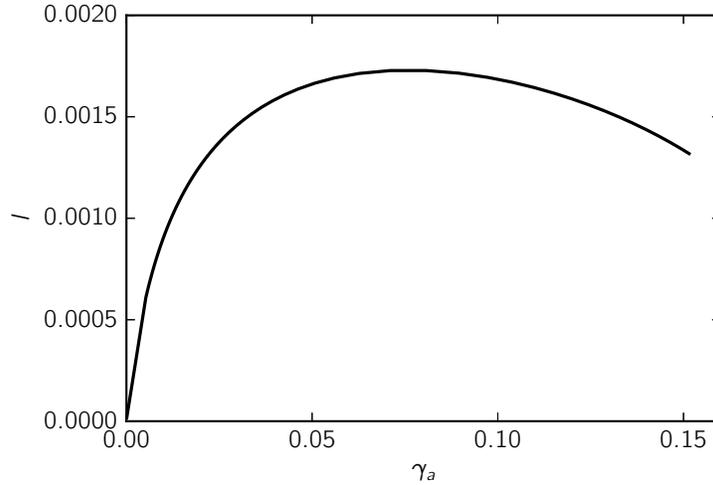
18

Figure 10: Output current l versus out coupling strength γ_a at stable equilibria.

of output currents. (See Figure 11)

4   Improvements on previous analysis

Previously, the analysis done by Zozulya and Anderson [2013] has found steady state solutions for low output. However, the behavior of the system in the critical region is still unknown, that is, what kind of behavior the system exhibits in the region where there was no steady state for the chemical potential μ_a but μ_{ex} has not reached zero yet. More intuitively, we want to be able to explain the reason why in Figure 12, the left branch of the dashed curve ends before the chemical potential of the BEC reaches zero, which is what we would expect from the critical situation, when BEC is about to be completely drained.

To answer this question, first we plot the μ_a-l curve, highlighting the new stable steady states that are previously unknown. In Figure 13 we see that the critical point where the BEC is completely drained does not occur at a maximal output current. In fact we can keep increasing out coupling,
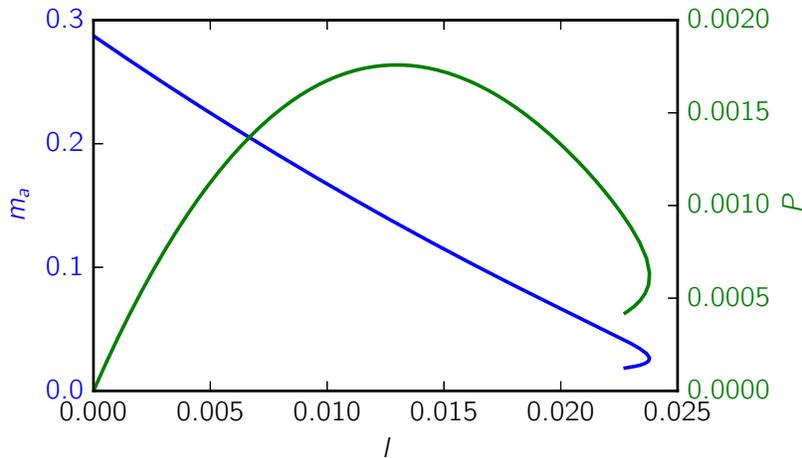
Figure 11: Current (l) voltage (m_a) relation of the battery (blue line), and power output (P) at different load voltage (green line), with $i = 2.0$.

and see a consequent decrease of l, and finally the destabilization of the system. This also means that there can be no physically achievable solution that produces a higher outcoupling current.

In addition, we have also been able to assess the stability of the steady states of the system, which is unknown before. We have found that all the solutions that were found by Zozulya and Anderson [2013] are stable, and there are in fact additional stable equilibria. Unstable equilibria also exist, but for practical purposes, we shall not consider the output of the battery at those solutions.

The reason why we are able to obtain these additional solutions is that we used γ_a instead of l as the free parameter in the system. A physical justification of this choice is that γ_a is a more directly physical quantity, adjustable through the out-coupling mechanism, and since the relation between γ_a and I_l can be non-monotone, for a given output current, there may be multiple possible underlying state of the system, which is in fact the case, as we have seen from above calculations.

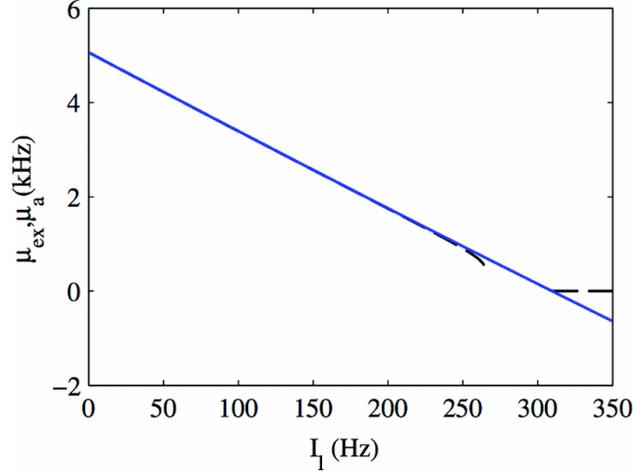A computation reason why using γ_a is better can be illustrated by plotting the bifurcation

Figure 12: Chemical potential of thermal atoms μ_{ex} (solid line) and the condensate μ_{a} (dashed line) versus load current [Zozulya and Anderson, 2013]

diagrams against l. From Figure 14, we can see that in the two branches of solutions almost overlap in the τ and n_{ex} diagrams. This means that if we attempted to perform the bifurcation analysis with respect to l, then the numerical methods would likely not have enough precision to distinguish between the two branches of solutions, and report a singularity near the maximum of
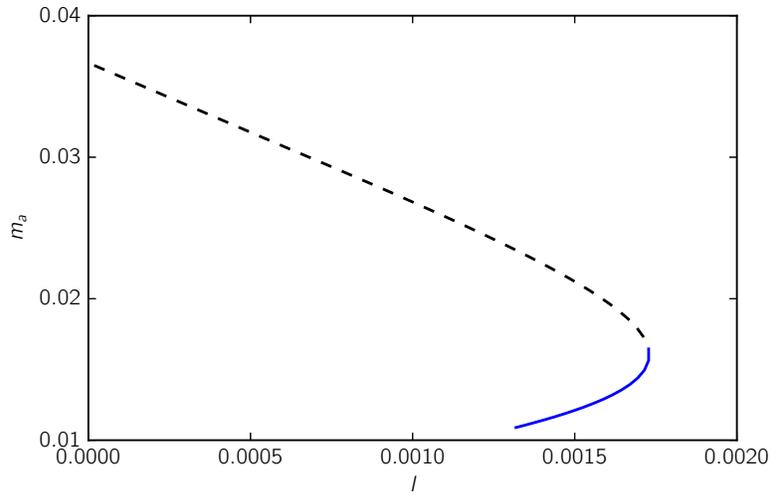

Figure 13: Previously found i-v characteristic (dashed line) and newly found i-v characteristic.
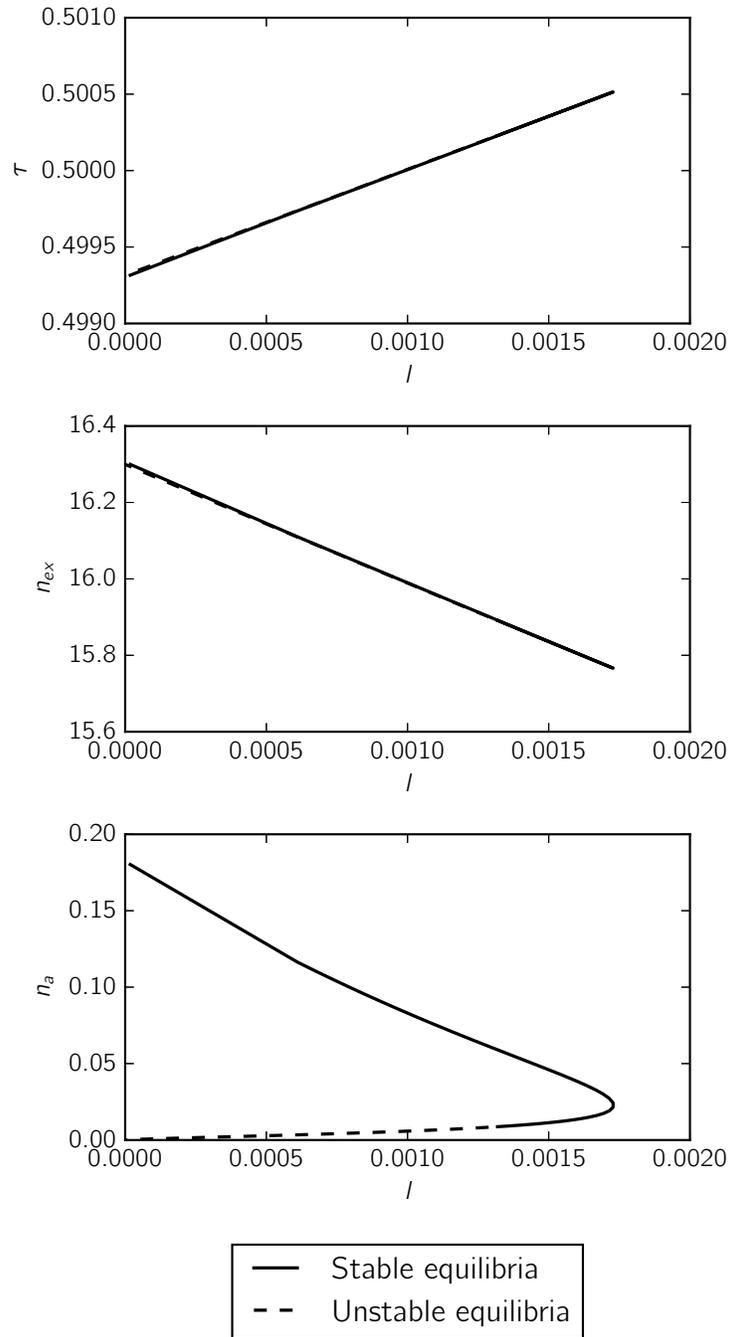
Figure 14: Bifurcation diagram of the state variables τ, n_{ex}, and n_a.

l, which is what happened in previous analysis.

5   Conclusion

In this project we have analyzed the atomtronic battery model conceived by Zozulya and Anderson [2013]. The model consists of cold atoms trapped in an asymmetric potential well, loaded continuously while having Bose-Einstein condensate outcoupled from it. The trap can be characterized by its frequencies and heights in each direction, with the longitudinal frequency f_z being much smaller than the transverse frequency $f_\perp$. The trap heights U_z and $U_\perp$ can be adjusted so that atoms carrying a select range of energy are allowed to escape, which combined with the continuous loading of cold atoms can effectively cool down the trap.

We calculated the steady states and bifurcations of this system, and analyzed the stability of such steady states. Using these data, we have extended the analysis provided by Zozulya and Anderson [2013], and provided a full account of the characteristics of this model as a battery. We have solved the question raised about the behavior of the system in the critical region, and reassured that the solutions are indeed stable and experimentally possible.

Appendices

A   Code used in computation

Fortran equation script used in AUTO:

```
!----------------------------------------------------------------------
!----------------------------------------------------------------------
!   atb :      The atomtronic battery
!----------------------------------------------------------------------
!----------------------------------------------------------------------

SUBROUTINE FUNC(NDIM,U,ICP,PAR,IJAC,F,DFDU,DFDP)
!      ---------- ----

      IMPLICIT NONE
      INTEGER, INTENT(IN) :: NDIM, ICP(*), IJAC
      DOUBLE PRECISION, INTENT(IN) :: U(NDIM), PAR(*)
      DOUBLE PRECISION, INTENT(OUT) :: F(NDIM)
      DOUBLE PRECISION, INTENT(INOUT) :: DFDU(NDIM,NDIM), DFDP(NDIM,*)

      DOUBLE PRECISION ga, x, y, z, temp, na, nex, exp1, exp2, exp3, &
      tempsq, tempnafac, tna15, tna25, tna35, tna45, rhs1, rhs2, rhs3, &
      dfdu11, dfdu12, dfdu13, dfdu21, dfdu22, dfdu23, dfdu31, dfdu32, dfdu33, &
      a, b, dadx, dady

!      Helper variables

      ga=PAR(1)
      x = U(1)
      y = U(2)
      z = U(3)

      temp = 0.49931569561007d0+x
      nex = 16.29956107597423d0+y
      na = 0.18024048804064646d0+z

      exp1 = exp(2.4006428571428566d0/temp)
      exp2 = exp(6.5435d0/temp)
      exp3 = exp(4.142857142857143d0/temp)

      tempsq = temp*temp
```

24

```fortran
      tempnafac = (1428.5714285714284d0*tempsq*na)/exp1
      tna15 = (na+tempnafac)**0.2d0
      tna25 = (na+tempnafac)**0.4d0
      tna35 = (na+tempnafac)**0.6d0
      tna45 = (na+tempnafac)**0.8d0

      a = 6.576866724612946d0*nex - (454.0880804015761d0*temp*temp*temp)/ &
            (1d0 + 0.1912677944123304d0*temp)
      b = 6.576866724612946d0*temp
      dadx = -3d0*454.0880804015761d0*tempsq/(1d0 + 0.1912677944123304d0*temp)+ &
            (454.0880804015761d0*temp*temp*temp)/(1d0 + &
            0.1912677944123304d0*temp)**2*0.1912677944123304d0
      dady = 6.576866724612946d0

!     Right hand sides of the dynamic equations

      rhs1=9.836413718796749d0+((-236294.92486093647d0+ &
            exp1*(-491.79884533385075d0-255.09732347149122d0*x)+ &
            x*(-1.0091350398218739d6+(-1.198755626226754d6- &
            251327.41228718346d0*x)*x))*nex)/ &
      exp2+(0.15301182606334032d0*na* &
            tna45*(-0.1462508606594111d0*nex+ &
            tempsq*(17.408285516201083d0*temp+tna25)))/temp

      rhs2=1.3966510351232706d0-(87.96459430051422d0*nex)/ &
      exp3-(125663.70614359173d0*tempsq*nex)/ &
            exp2+(na* &
            tna25*(-0.5330928992224307d0*nex+ &
            tempsq*(63.454213906715296d0*temp+3.645058202179727d0*tna25)))/ &
            temp

      rhs3=(na*(-ga*temp+ &
            tna25*(0.5330928992224309d0*nex+ &
            tempsq*(-63.45421390671528d0*temp- &
            3.645058202179727d0*tna25))))/temp

      F(1) = (rhs1 - b*rhs2)/a

      F(2) = rhs2

      F(3) = rhs3

!     Jacobian of the equation

      IF(IJAC.EQ.0)RETURN
```

```
dfdu11=(-255.0973234714912d0*exp1* &
      exp1*(8.236277106920209d0+5.141488534077284d0*x+x*x)*nex* &
      tna15-753982.2368615504d0*exp1* &
      tempsq*(9.563729708365564d0+5.360964724553473d0*x+x*x)*nex* &
      tna15+exp1*exp2* &
      na*na*(0.022378111252831633d0*nex+ &
      tempsq*(5.3273471109318535d0*temp+0.15301182606334032d0*tna25))+ &
      exp2*temp* &
      na*na*(-19.181238216712824d0*(3.7001728384672123d0+x)*nex+ &
      13698.892570967622d0* &
      tempsq*(0.5156891990215973d0+1.5321075816963303d0*x+x*x+ &
      0.07305660395295867d0*tna25+ &
      0.05425258240195416d0*x*tna25)))/(exp1*exp2*tempsq*tna15)

dfdu21=(-364.4247478164161d0*exp1*exp2*nex*tna35- &
      251327.41228718346d0*exp2*tempsq*(3.7710656956100705d0+x)*nex* &
      tna35+exp2*exp2* &
      na*na*(0.5330928992224309d0*nex+ &
      tempsq*(126.90842781343058d0*temp+3.645058202179727d0*tna25))+ &
      exp3*exp3*exp1*temp* &
      na*na*(152.3122569206945d0*(-4.301970018675643d0+x)*nex+ &
      253816.8556268612d0* &
      tempsq*(0.4205559721862297d0+1.3415803708119767d0*x+x*x+ &
      0.06603454699169665d0*tna25+ &
      0.0533407742943583d0*x*tna25)))/(exp2*exp2*tempsq*tna35)

dfdu31=(na*na &
      *(exp1*(-0.5330928992224309d0*nex+ &
      tempsq*(-126.9084278134306d0*temp- &
      3.6450582021797273d0*tna25))+ &
      temp*(-152.3122569206945d0*(-4.301970018675645d0+x)*nex- &
      253816.85562686116d0* &
      tempsq*(0.4205559721862297d0+1.3415803708119767d0*x+ &
      x*x+0.06603454699169668d0*tna25+ &
      0.05334077429435831d0*x*tna25))))/(exp1*tempsq*tna35)

dfdu12=(-491.79884533385075d0-255.09732347149122d0*x)/ &
exp3-(251327.41228718346d0*tempsq*(3.7710656956100697d0+x))/ &
exp2-(0.022378111252831633d0*na*tna45)/temp

dfdu22=-87.96459430051422d0/exp3-(125663.70614359173d0*tempsq)/ &
exp2-(0.5330928992224307d0*na*tna25)/temp

dfdu32=(0.5330928992224309d0*na*tna25)/temp
```

```fortran
dfdu13=(na*(-57.543714650138476d0*tempsq*nex+ &
      tempsq*tempsq*(6849.44628548381d0*temp+ &
      480.8943104847838d0*tna25)+ &
      exp1*(-0.040280600255096936d0*nex+ &
      tempsq*(4.794612399838668d0*temp+ &
      0.3366260173393487d0*tna25))))/(exp1*temp*tna15)

dfdu23=(na*(-1066.1857984448613d0*tempsq*nex+ &
      tempsq*tempsq*(126908.4278134306d0*temp+ &
      9373.006805605013d0*tna25)+ &
      exp1*(-0.7463300589114031d0*nex+ &
      tempsq*(88.83589946940141d0*temp+ &
      6.561104763923509d0*tna25))))/(exp1*temp*tna35)

dfdu33=(tempsq* &
      na*(1066.1857984448618d0*nex+ &
      tempsq*(-126908.42781343055d0*temp-9373.006805605013d0*tna25))+ &
      exp1*(0.7463300589114032d0*nex*na+ &
      temp*(-ga*tna35+ &
      temp*na*(-88.8358994694014d0*temp- &
      6.5611047639235105d0*tna25))))/(exp1*temp*tna35)


DFDU(1,1) = (dfdu11-b*dfdu21-6.576866724612946d0*rhs2)/a-F(1)/a*dadx

DFDU(2,1) = dfdu21

DFDU(3,1) = dfdu31

DFDU(1,2) = (dfdu12-b*dfdu22)/a-F(1)/a*dady

DFDU(2,2) = dfdu22

DFDU(3,2) = dfdu32

DFDU(1,3) = (dfdu13-b*dfdu23)/a

DFDU(2,3) = dfdu23

DFDU(3,3) = dfdu33


IF(IJAC.EQ.1)RETURN
```

```fortran
      DFDP(1,1) = 0.0d0
      DFDP(2,1) = 0.0d0
      DFDP(3,1) = - na



END SUBROUTINE FUNC

SUBROUTINE STPNT(NDIM,U,PAR,T)
!        ---------- -----

      IMPLICIT NONE
      INTEGER, INTENT(IN) :: NDIM
      DOUBLE PRECISION, INTENT(INOUT) :: U(NDIM),PAR(*)
      DOUBLE PRECISION, INTENT(IN) :: T

      PAR(1)=0.0d0

      U(1)=0.0d0
      U(2)=0.0d0
      U(3)=0.0d0

END SUBROUTINE STPNT

SUBROUTINE BCND
END SUBROUTINE BCND

SUBROUTINE ICND
END SUBROUTINE ICND

SUBROUTINE FOPT
END SUBROUTINE FOPT

SUBROUTINE PVLS
END SUBROUTINE PVLS
```

Python script used to run the continuation in AUTO:

```python
#==============
# AUTO run atb
#==============

print "\n***Compute a family of stationary solution"
```

```
atb=run('atb',JAC=1,PAR={'ga':0.0001},NMX=500,DSMAX=0.01)
save('atb')

print "\n***Compute the periodic solution family***"
run(atb('HB1'), IPS=2, ICP=['ga','PERIOD'],ILP=0,NMX=50,
    NPR=2,DS=0.01,DSMIN=0.005,DSMAX=0.1,
    UZSTOP={'ga': [0.14,0.17], 'PERIOD': [0, 1e4]})
save('atbps')
append('atb')

print "\n***Clean the directory***"
clean()
```

References

E. A. Cornell and C. E. Wieman. Nobel lecture: Bose-einstein condensation in a dilute gas, the first 70 years and some recent experiments. *Rev. Mod. Phys.*, 74:875–893, Aug 2002. doi: 10.1103/RevModPhys.74.875.

E. J. Doedel and B. E. Oldeman. Auto-07p: Continuation and bifurcation software for ordinary differential equations. January 2012. URL http://www.dam.brown.edu/people/sandsted/auto/auto07p.pdf.

J. G. Lee, B. J. McIlvain, C. Lobb, and W. Hill III. Analogs of basic electronic circuit elements in a free-space atom chip. *Scientific reports*, 3, 2013.

R. Pathria and P. Beale. *Statistical Mechanics*. Elsevier Science, 2011. ISBN 9780123821898.

R. A. Pepino, J. Cooper, D. Z. Anderson, and M. J. Holland. Atomtronic circuits of diodes and transistors. *Phys. Rev. Lett.*, 103:140405, Sep 2009. doi: 10.1103/PhysRevLett.103.140405.

C. Pethick and H. Smith. *Bose-Einstein Condensation in Dilute Gases*. Cambridge University Press, 2002. ISBN 9780521665803.

C. F. Roos, P. Cren, D. Guéry-Odelin, and J. Dalibard. Continuous loading of a non-dissipative atom trap. *EPL (Europhysics Letters)*, 61(2):187, 2003.

J. Sakurai and J. Napolitano. *Modern Quantum Mechanics*. Pearson Education, 2014. ISBN 9780321972071.

B. T. Seaman, M. Krämer, D. Z. Anderson, and M. J. Holland. Atomtronics: Ultracold-atom analogs of electronic devices. *Phys. Rev. A*, 75:023615, Feb 2007. doi: 10.1103/PhysRevA.75. 023615.

J. A. Stickney, D. Z. Anderson, and A. A. Zozulya. Transistorlike behavior of a bose-einstein condensate in a triple-well potential. *Phys. Rev. A*, 75:013608, Jan 2007. doi: 10.1103/PhysRevA. 75.013608.

A. A. Zozulya and D. Z. Anderson. Principles of an atomtronic battery. *Physical Review A*, 88(4): 043641, 2013.